Filtering Drifter Trajectories Sampled at Submesoscale Resolution

Max Yaremchuk and Emanuel F. Coelho

***Abstract*—In this paper, a variational method for removing positioning errors (PEs) from drifter trajectories is proposed. The technique is based on the assumption of statistical independence of the PEs and drifter accelerations. The method provides a realistic approximation to the probability density function of the accelerations while keeping the difference between the filtered and observed trajectories within the error bars of the positioning noise. Performance of the method is demonstrated in application to real data acquired during the Grand Lagrangian Deployment (GLAD) experiment in the Northern Gulf of Mexico in 2012.**

***Index Terms*—Computers and information processing/data processing, mathematics/filtering algorithms, optimization, smoothing methods.**

I. Introduction

STUDIES of the world ocean with Lagrangian floats have a long history [24]. Drifters were mostly employed for the exploration of the large-scale [25], [19], [7], [26] and mesoscale [9], [27] circulations with typical intervals between the drifter position fixes $\boldsymbol{r}(t_n)$ ranging from 1 h to ten days.

In recent years, there has been a growing interest in the analysis of the Lagrangian coherent structures and submesoscale processes at the ocean surface (e.g., [3], [23], [11], and [4]), fueled by the necessity to increase the efficiency of oil spill management, search-and-rescue missions, and ecological control.

The Lagrangian studies at submesoscale resolution require position sampling interval δt as small as several minutes, which amplifies noise in the estimates of drifter accelerations

$$\boldsymbol{a}(t_n) = [\boldsymbol{r}(t_{n-1}) - 2\boldsymbol{r}(t_n) + \boldsymbol{r}(t_{n+1})]\delta t^{-2} \tag{1}$$

to a level comparable with the accelerations experienced by the drifters. Assuming stationarity and statistical independence of the positioning errors (PEs), (1) yields the following estimate of the PE-induced acceleration error:

$$\sigma_p = \sqrt{6}\sigma_e \delta t^{-2}. \tag{2}$$

For a sampling interval $\delta t = 5$ min and a positioning error $\sigma_e = 1.5$ m, the acceleration error is $\sigma_p = 4 \times 10^{-5}$ m/s^2, a value comparable with the typical Coriolis acceleration of a water parcel moving at the speed of 2 m/s in midlatitudes. On the other hand, a typical acceleration of submesoscale motions in the surface layer estimated as U^2/L has similar magnitude for a characteristic velocity U and horizontal L scales of 0.2 m/s and 1 km, respectively (e.g., [28]). At the same time, submesoscale phenomena are characterized by significant horizontal intermittency, because their growth and development are associated with mechanisms (frontogenesis, mixed-layer instabilities) requiring specific environmental conditions (strong subsurface stratification and/or horizontal velocity shear). The intermittent nature of submesoscale turbulence implies that the acceleration probability density function (pdf) may have long tails and a sharp peak in the region of small ($a < 10^{-5}$ m/s^2) accelerations corresponding to the geostrophically balanced flows with typical velocities of 0.1–0.2 m/s.

Accurate estimates of the Lagrangian accelerations in the geophysical flows are important for the model skill improvement because they provide information on the actual forces acting within the fluid. In addition, the Lagrangian point of view is in many aspects the most natural way to obtain understanding of the turbulent transport and mixing. For these reasons, there has been a substantial progress in both experimental [13], [31], [18] and theoretical [12], [5], [16] studies of the submesoscale structures in the past decade.

Currently, high-resolution satellite images provide the best observational window into the submesoscale world. Developments of the towed platforms and autonomous underwater vehicle technology also contribute to the rapid increase of the experimental data at submesoscale. In the recent work of Gaultier *et al.* [10], the first attempt has been made to correct surface velocity field using submesoscale sea surface temperature. Drifter trajectories, sampled at temporal resolution $\delta t \sim L/U \ll 90$ min, constitute another valuable source of information on submesoscale dynamics. The recent Grand Lagrangian Deployment (GLAD) experiment conducted in the Gulf of Mexico in 2012 appears to be the first experimental study of submesoscale processes using a massive array of several hundred Lagrangian drifters.

Manuscript received February 19, 2014; revised August 07, 2014; accepted August 21, 2014. Date of publication October 21, 2014; date of current version July 10, 2015. This work was supported by a grant from The Gulf of Mexico Research Initiative through the Consortium for Advanced Research on Transport of Hydrocarbon in the Environment (CARTHE).

Associate Editor: J. F. Lynch.

M. Yaremchuk is with the Naval Research Laboratory, Stennis Space Center, MS 39556 USA.

E. F. Coelho is with the Marine Sciences Department, University of Southern Mississippi, Stennis Space Center, MS 39522 USA (e-mail: emanuel.coelho.ctr.po@nrlssc.navy.mil).

Digital Object Identifier 10.1109/JOE.2014.2353472

In this paper, we propose a variational algorithm for filtering measurement errors from drifter coordinates acquired at temporal resolution high enough to contaminate the statistics of accelerations caused by physical processes in the upper ocean. Since the typical PE magnitude σ_e is small compared to the distance between the drifter position fixes, PEs have a small impact on the Lagrangian velocity statistics, but distort considerably the statistics of Lagrangian accelerations. For this reason, the proposed filtering method is based on the assumption that PEs are statistically independent of the Lagrangian accelerations whose pdf is employed for regularization of the cost function.

The paper is organized as follows. In Sections II and III, we describe the method and the data used for its validation. In Section IV, the method is applied to drifter trajectories documented during the GLAD experiment. The results are summarized and discussed in Section V.

II. Method

Assuming that drifter accelerations $\boldsymbol{a}$ and errors $\boldsymbol{e}$ in measuring drifter coordinates are statistically independent, their joint (prior) pdf $P(\boldsymbol{a},\boldsymbol{e})$ is

$$P(\boldsymbol{a},\boldsymbol{e}) = P_a(\boldsymbol{a})P_e(\boldsymbol{e}). \tag{3}$$

Consider N random $2d$ vectors $\boldsymbol{a}_n$ and $\boldsymbol{e}_n$, $n = 1,\dots,N$, and assume that P_e can be approximated by the Gaussian distribution, so that

$$P_e(\boldsymbol{e}_1,\dots,\boldsymbol{e}_N) \propto \exp\left[-\frac{1}{2}\sum_{n=1}^{N}\frac{\boldsymbol{e}_n^2}{\sigma_n^2}\right] \tag{4}$$

where σ_n are the root mean square (rms) PE variances. In addition, we assume that the prior pdf for accelerations P_a can be represented by the stretched exponential law, a particular case of the q-exponential distribution with $q = 1$, often used to describe statistics of the Lagrangian accelerations in turbulent flows (e.g., [1])

$$P_a(\boldsymbol{a}_1,\dots,\boldsymbol{a}_n) \propto \exp\left[-\sum_{n=1}^{N}\frac{(\boldsymbol{a}_n^2)^{\mu}}{(a^2)^{\mu}}\right] \tag{5}$$

where μ is the adjustable parameter defined in Section IV.

Let us also assume that additional information on $\boldsymbol{a}$ and $\boldsymbol{e}$ is available in the form of the observed drifter positions $\boldsymbol{r}_n^*$ and the deterministic relationships (1) and $\boldsymbol{e}_n = \boldsymbol{r}_n - \boldsymbol{r}_n^*$, with $\boldsymbol{r}_n$ being the unknown true position at time t_n. Substitutions of these constraints into (3) transforms it into the posterior pdf P^* written in terms of $\boldsymbol{r}$

$$P^*(\boldsymbol{r}) \propto \exp\left[-\sum_{n=2}^{N-1}\frac{(\boldsymbol{r}_{n+1}-2\boldsymbol{r}_n+\boldsymbol{r}_{n-1})^{2\mu}}{(\delta t^2 a)^{2\mu}} - \sum_{n=1}^{N}\frac{(\boldsymbol{r}_n-\boldsymbol{r}_n^*)^2}{2\sigma_n^2}\right]. \tag{6}$$

The pdf (6) can be also obtained using the well-known Bayesian approach under the standard assumption of an improper prior (e.g., [14]).

The most likely drifter trajectory can be found by maximizing the probability $P^*[\boldsymbol{r}]$ in the $2N$-dimensional space of unknown true positions $\boldsymbol{r}_n$, or by minimizing the following cost function:

$$J = \sum_{n=2}^{N-1} W_a(\boldsymbol{r}_{n+1}-2\boldsymbol{r}_n+\boldsymbol{r}_{n-1})^{2\mu} + \sum_{n=1}^{N} W_n(\boldsymbol{r}_n-\boldsymbol{r}_n^*)^2 \to \min_{\boldsymbol{r}_n} \tag{7}$$

where $W_n = \sigma_n^{-2}/2$ and $W_a = (\delta t^2 a)^{-2\mu}$.

Since the true acceleration variance σ_a^2 is unknown, the value of W_a is still undefined. However, it can be expressed in terms of the directly measured quantities: observed acceleration variance σ_*^2 and the acceleration variance σ_p^2 induced by PEs (2). Because PEs and accelerations are statistically independent, then

$$\sigma_*^2 = \sigma_p^2 + \sigma_a^2 \tag{8}$$

and, combining (8) with the linear relationship between σ_a^2 and a^2, one can obtain

$$W_a = (\delta t^2 a)^{-2\mu} = [C\delta t^4(\sigma_*^2 - \sigma_p^2)]^{-\mu} \tag{9}$$

where C is the proportionality coefficient (see the Appendix).

Given the statistical model (6), the minimization problem (7) and (9) has the only free parameter μ, which can be optimized by choosing its value such that the rms difference between the most likely and observed drifter trajectory is equal to the magnitude of the Global Positioning System (GPS) noise.

Numerically, the cost function (7) is minimized using the double-precision version of the quasi-Newtonian descent algorithm of Gilbert and Lemarechal [9]. The high machine precision is essential because trajectory lengths are several orders in magnitude larger than the GPS errors. In the real application described below, the algorithm converged rather quickly and required less than a hundred iterations to process a trajectory. The total central processing unit (CPU) time needed for GLAD data filtering (few million position fixes) never exceeded 2 min on a laptop.

III. Data

A. The GLAD Experiment

In summer/fall 2012, an extensive Lagrangian experiment was conducted in the northern Gulf of Mexico. An array of 319 surface drifters was deployed in late July 2012, and the majority of drifters persisted throughout October 2012, a limitation imposed by their battery life. The deployed SPAR-type drifters were different from those traditionally used as part of the global drifter program. They were similar to the surface drifters (e.g., [8] and [22]) of the Coastal Ocean Dynamics Experiment (CODE), originally designed to follow the near surface upper-ocean flows in the presence of wind and waves. As such, the GLAD drifters were drogued at a depth of approximately 1 m to decouple their motion from direct wind forcing (estimated 1%–3% windage [9]) and damp-wave-induced motions without introducing a wave-phase-related bias [9]. Positions were reported at 5-min intervals, although significant data gaps occurred mostly due to adverse weather conditions, which required careful data processing to produce accurate trajectory and velocity estimates.

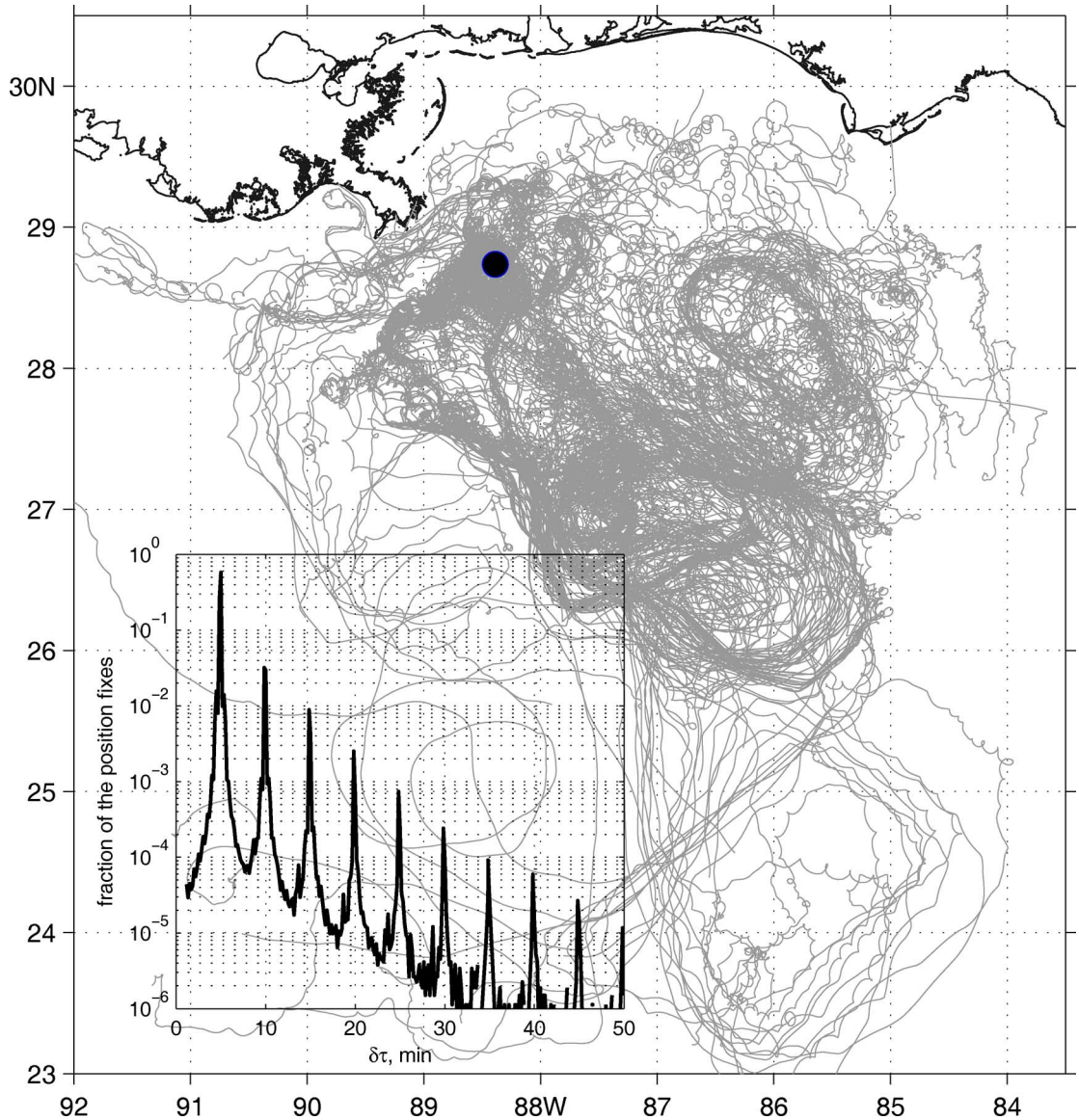

Fig. 1. Trajectories of the GLAD drifters (shown in gray, every second trajectory is given). The black circle depicts the location of the Deep Water Horizon oil spill. The distribution of the time intervals between the drifter position fixes is given in the inset.

The experiment constituted an essential first step to study pollutant transport by surface currents and explore interactions between mesoscale and submesoscale processes (Fig. 1). The major objective of the study was to improve understanding of the surface transport phenomena in the open ocean and near-coastal regions with an ultimate goal of improving Lagrangian predictability and dispersion of pollutants at time scales from a few hours to several weeks.

To address such a wide spectrum of temporal scales, the drifters were equipped with Secure POsiTioning (SPOT, http://www.findmespot.com) devices that recorded drifter positions every $\overline{\delta t} = 316$ s on average. Overall, more than 5×10^6 position fixes were registered with the total duration of the drifter trajectories of 49.2 years. The drifters were drogued at the average depth of 1 m and were released in a variety of clusters to explore a wide range of spatial scales (see [21] and www.carthe.org/research.php for details). In this paper, we focus on the analysis of drifter trajectories with an objective to remove SPOT positioning errors and improve the estimates of the drifters' accelerations.

Although the time intervals between the position fixes were not constant, the majority of them (85%) were within several seconds of $\delta t = 5$ min (inset in Fig. 1), with the multiples of δt corresponding to another 14% of the total number. The average distance between the sequential position fixes was close to 115 m, providing the mean drifter velocity of 0.36 m/s. These numbers show that even at such a short sampling time interval, PEs of several meters introduce velocity errors of a few centimeters per second, which is acceptable for most of the applications. In contrast, errors in drifter accelerations appear to be quite substantial [see (2)] with the magnitude several times larger than the typical magnitude of water acceleration in surface layer. Despite the high level of acceleration noise introduced by the GPS errors at such a high temporal resolution, the task of filtering this noise becomes feasible because the PE statistics can be assessed with a reasonable degree of accuracy.

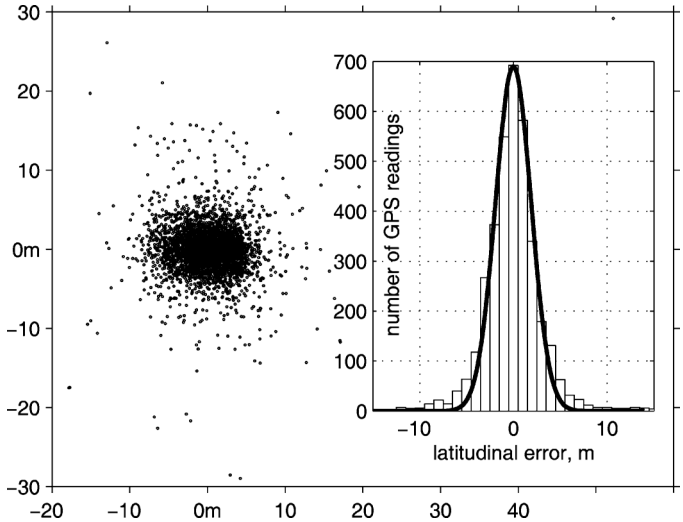

Fig. 2. Scatter plot of the coordinates of the drifter 309 while it was still on shore. Approximation of its meridional PE by the Gaussian pdf is shown in the inset.

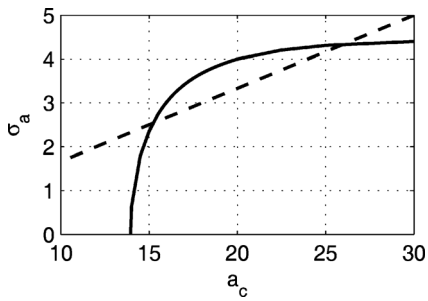

Fig. 3. Relationships between σ_a and a_c used for identification of the cutoff acceleration. The acceleration values (ms^{-2}) are multiplied by 10^5.

B. Positioning Errors

Among more than five million position fixes available in the GLAD database, a certain number were made from drifters that were not yet deployed did not change their location. In particular, the stationary position of the drifter 309 was recorded for more than two weeks (4980 position fixes) while it was on board of the docked deployment vessel at 29.3886 °N 90.7145 °W. This allowed us to assess the statistics of PEs under the undisturbed ashore conditions (Fig. 2).

In the first approximation, the PE distribution can be described by the uncorrelated Gaussian pdfs with the variances of $\sigma_x = 2.1$ and $\sigma_y = 1.9$ m in the zonal and meridional directions, respectively ($\sigma_e = \sqrt{\sigma_x^2 + \sigma_y^2} = 2.8$ m). The PE-induced "acceleration" rms variance σ_p was computed using the recorded time variation of the drifter's coordinates and was found to be 7.6×10^{-5} ms^{-2}.

It is noticeable that the pdf in Fig. 2 exhibits significant non-Gaussian tails for the errors exceeding 5 m. Accurate fitting of these tails by commonly used analytic functions (e.g., stretched exponentials) is impossible because of the insufficient statistics. Moreover, these tails are likely caused by random events (e.g., a sudden persistent decrease in the number of satellites) whose statistics are difficult to model.

To account for these tails, we elected a nonlinear approach: if the trajectory $\boldsymbol{r}(t)$ experienced a sudden excursion causing a large spike in acceleration, the PE error variance was inflated as follows:

$$\sigma_n = \sigma_e[1 + \gamma_n^2 \theta(\gamma_n - 1)], \qquad \gamma_n = \frac{\boldsymbol{a}_n^2}{a_c^2} \tag{10}$$

where a_c is the cutoff acceleration and θ is the step function. In actual computations, the relationship between $\boldsymbol{a}$ and $\boldsymbol{r}$ was modified to account for variations of the time intervals between the position fixes

$$\boldsymbol{a}_n = \frac{(\boldsymbol{r}_{n+1} - \boldsymbol{r}_n)\delta t_n^{-1} - (\boldsymbol{r}_n - \boldsymbol{r}_{n-1})\delta t_{n-1}^{-1}}{\frac{(\delta t_n + \delta t_{n-1})}{2}}. \tag{11}$$

The parameter a_c can be computed by taking into account the statistical independence of the PEs and drifter accelerations and considering limitations on the estimates of the acceleration probability density in the tails, imposed by the finite volume of the GLAD data. First, σ_a can be estimated from (8), (10), and (11) as a function of a_c, given the observed values of $\sigma_* = 8.9 \times 10^{-5}$ ms^{-2} and $\sigma_p = 7.6 \times 10^{-5}$ ms^{-2}. With the decrease of a_c, the value of σ_p^2 increases as more points on the trajectory are treated as outliers and penalized by large observation variance according to (10). As a consequence, the value of $\sigma_a = \sqrt{\sigma_*^2 - \sigma_p^2(a_c)}$ decreases until it reaches zero at $a_c = 1.39 \times 10^{-4}$ ms^{-2}. This dependence is shown by the solid line in Fig. 3. The second relationship between σ_a and a_c can be obtained by considering the limitation in the assessment of the acceleration statistics: With the finite number of samples M, the remote ($a \gg a_c$) structure of the pdf tails cannot be adequately resolved if these tails are described by less than a few hundred samples, i.e., $M\mathcal{P}_a(a \gg a_c) \simeq 10^2$. Using the analytic pdfs describing the experimental data on the Lagrangian accelerations, e.g., [1] and [2], it is possible to estimate that for several million GLAD samples the cutoff value can be reasonably constrained by $a_c = 6\sigma_a$ (a dashed line in Fig. 3). Among the two roots visible in Fig. 3, we used the smaller one, primarily because the larger cutoff value identified too few spikes as outliers.

One should note that for a deployed drifter the value of σ_p should be larger than 7.6×10^{-5} $\mathrm{m/s}^2$ because of the additional factors causing the loss of sight of GPS satellites. However, in view of (8), the (hardly measurable) increase in σ_p is constrained from above by the value of the observed drifter acceleration σ_*. In the case of GLAD data, this increase can be considered as negligible in the first approximation because the value of $\sigma_a = (\sigma_*^2 - \sigma_p^2)^{1/2} = 4.5 \times 10^{-5}$ $\mathrm{m/s}^2$ appears to be fairly consistent with the typical accelerations of the drifters involved in submesoscale motions.

As a result of PE analysis of the GLAD data, the cost function was modified to account for non-Gaussian tails in the PE distribution. The modification allows PE variances to change in time through parameterization (10) with the cutoff scale $a_c = 1.56 \times 10^{-4}$ ms^{-2}, corresponding to the Coriolis acceleration experienced by a water parcel traveling at a speed of 2.2 m/s. This value corresponds to the Rossby number $Ro = U/fL \sim 30$,

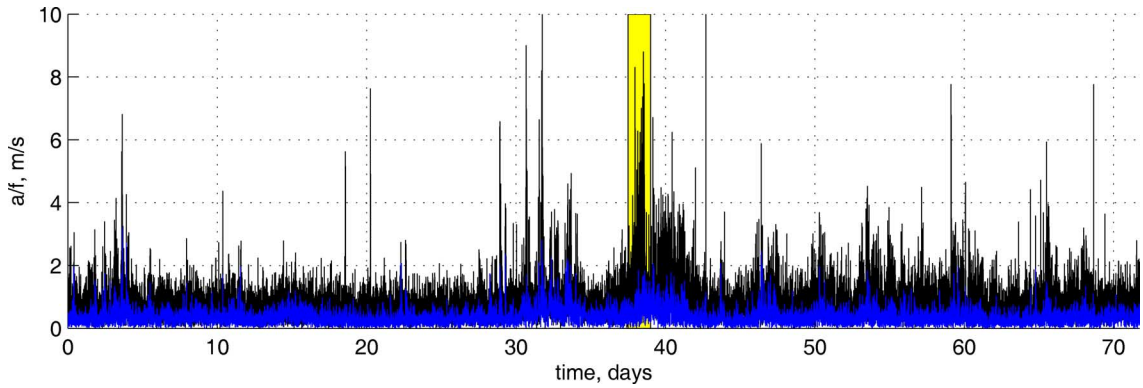

Fig. 4. Time evolution of the observed (black) and filtered (light blue) acceleration magnitude of a GLAD drifter trajectory. Yellow rectangle shows time interval corresponding to the piece of the trajectory exposed in Fig. 5(b)–(c). The magnitude of accelerations is divided by the mean Corioilis parameter $f = 7.3 \times 10^{-5}$ s^{-1}.

which is far beyond the typical range $0.5 < Ro < 5$ of submesoscale motions and, therefore, has a negligible impact on the acceleration statistics of submesoscale turbulence.

IV. Results

Before applying the filter to GLAD trajectories, the raw data were quality controlled. First, 12-h pieces of the trajectories were cut from both ends to remove time intervals when the drifters were on board before and immediately after the deployment. The trajectories with the maximum speeds exceeding 3 m/s and shorter than five days were also discarded. Finally, the trajectories with the maximum sampling time interval larger than 2 h and persistent (lasting more than $2\delta t$) zero accelerations were discarded to remove the impact of time extrapolation of the SPOT software in case when satellite signal was lost.

The filter was tuned by performing a series of filtering experiments with variable parameter μ. Statistically, the mean rms difference $\sigma_e = 2.8$ m between the raw and filtered drifter coordinates was achieved at $\mu = 0.91$ and this value was chosen as an optimal one for the filter. Interestingly, it is close to the one (0.90) obtained by Lewis and Swinney [15], for the distribution of the Lagrangian velocity increments in the turbulent flow.

In total, 169 trajectories with 2.4 million position fixes were filtered. Among those, 51 387 acceleration spikes were identified and 92% of them were reduced to a level below a_c after the PE correction of the trajectories. The remaining accelerations never exceeded $1.3a_c$.

A comparison of the raw and filtered trajectories is shown in terms of accelerations (Fig. 4) and actual coordinates (Fig. 5) for an arbitrarily selected drifter. During 2.5 months of the drifter operation, there were multiple events of enhanced accelerations lasting from several minutes to several days (Fig. 4). Of course, the origin of accelerations cannot solely be attributed to the GPS noise, because the drifters are also exposed to a wide range of unresolved small-scale phenomena such as sudden wind gusts, Langmuir cells, wave-induced Stokes drift, etc. However, according to the estimates in Section III, more than half of the acceleration variance (visible in black in Fig. 4) should be attributed to the GPS noise.

Fig. 5 provides a more detailed exposure of the filter's correction of the drifter's coordinates. Of particular interest are the abrupt changes between the periods of relatively uniform motion and periods of intense variations of the drifter position at the scales of less than a few kilometers [Fig. 5(a)]. Such behavior is indicative of intermittent nature of the submesoscale turbulence. The part of the trajectory, corresponding to the sequence of high acceleration events on day 38 visible in Fig. 4, is shown in Fig. 5(b). Because the resolution of Fig. 5(b) is still insufficient, Fig. 5(c) shows deviations of the trajectory from the uniform motion between its end points. An example of filtering the sudden coordinate excursion observed on day 42 (see acceleration peak exceeding $10f$ m/s^2) is demonstrated in Fig. 5(d). This event is likely to be caused by the GPS error because the drifter immediately returned to the original track. Random inspection of several events of this type has shown that the filter performed reasonably well.

The blue curve in Fig. 6 shows the pdf of the accelerations of the analyzed GLAD trajectories. In the region $|a| < 0.9a_c$, the pdf is virtually indistinguishable from the Gaussian noise parabola with the rms acceleration error variance corresponding to the positioning error of 2 m. This supports the validity of the PE model used in the formulation of the cost function (7). The clearly visible tails of the observed acceleration pdf stretch to the values of 3.5×10^{-4} m/s^2 and could be attributed to the non-Gaussianity of the error distribution in Fig. 2. They are removed by the filtering algorithm. The deviations of the filtered drifter positions from the observed ones rarely exceed several meters, and appear to be negligible compared to the spatial scales of the submesoscale motions [Fig. 5(a)]. However, the pdf of filtered accelerations has changed dramatically, and appears to be more realistic.

To support this statement, we calculated the pdf of the Lagrangian accelerations from the 1-km Navy Coastal Ocean Model (NCOM) simulation during the GLAD experiment. The virtual trajectories were computed by integrating the NCOM velocity field contaminated by a random walk process whose effective dispersion coefficient (150 m^2/s) was specified as the mean value of the Smagorinsky diffusion coefficient in the model run. The time integration was performed with the fourth-order Runge–Kutta scheme. Five million virtual drifter positions in more than a thousand randomly selected trajectories were sampled at 5-min resolution and processed to obtain

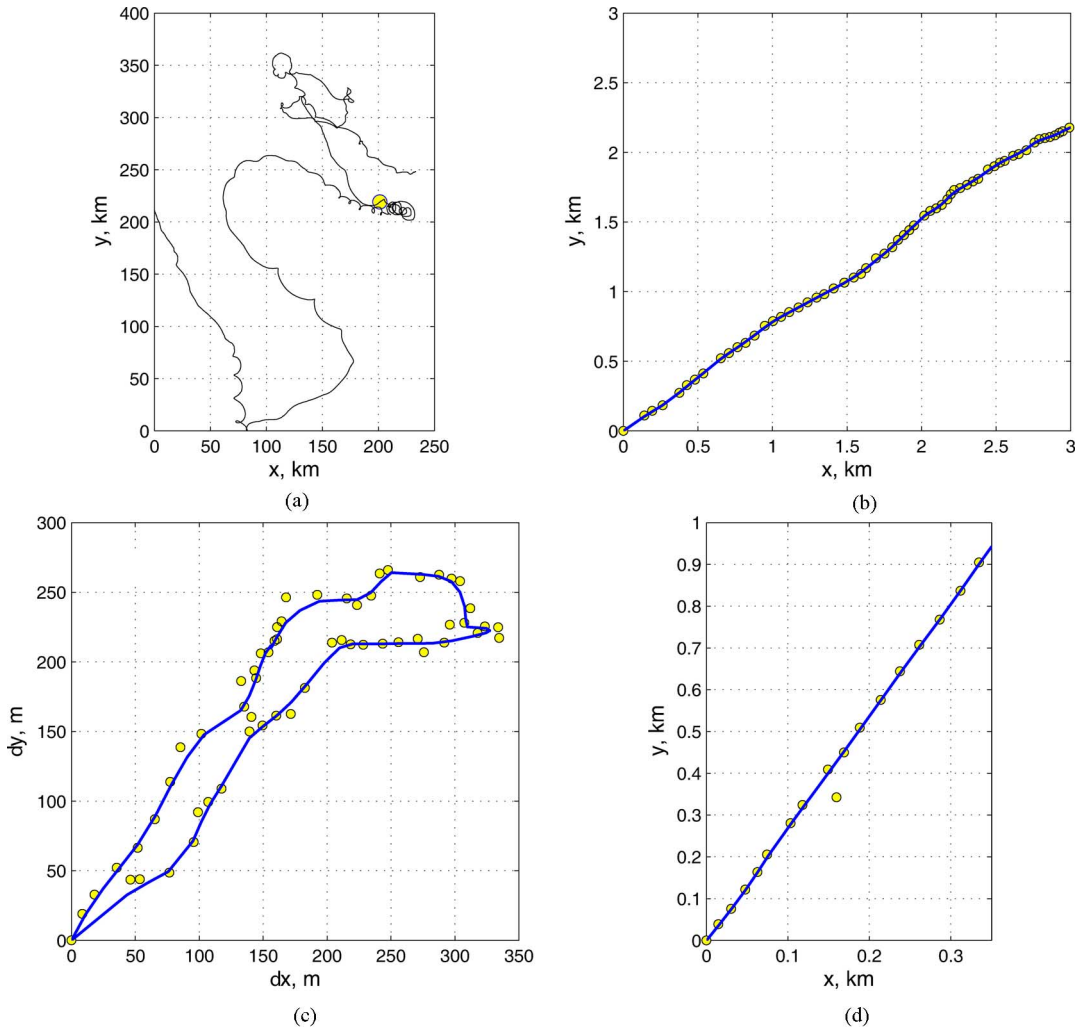

Fig. 5. Trajectory of a typical GLAD drifter relative to its mean position (a). The yellow circle shows the location of the trajectory part expanded in (b). Deviations of the trajectory in (b) from the uniform motion between the end points are shown in (c). Yellow circles show the observed positions, and the blue line is the filtered trajectory. Panel (d) is the same as in (b), but for the high-acceleration event on day 42.

the pdf shown in Fig. 6 by the light gray line, which fits the filtered pdf (the red line in Fig. 6) in a reasonably wide range of accelerations. It is also remarkable that the shape of the filtered pdf is qualitatively consistent with the typical pdfs of the Lagrangian accelerations observed in the laboratory experiments (e.g., [17] and [30]) and appears to be in a reasonable quantitative agreement with the log-normal superstatistics of the Lagrangian accelerations [2] shown by the dashed line in Fig. 6.

The impact of the filter on the correlation functions and spectra of the Lagrangian accelerations is shown in Fig. 7. The curves were obtained by averaging the trace of the autocorrelation matrix over the ensemble of the drifter trajectories for the delay times τ between 5 min and one month. The most severe contamination of the acceleration statistics by the GPS noise occurs at time scales close to the sampling interval, rendering the shape of sample autocorrelation to be close to the δ-function (a light gray curve in the inset of Fig. 7). After filtering, the autocorrelation exhibits a more realistic behavior, better visible in spectral representation: In contrast to the raw acceleration spectrum, which is close to white for the periods $T < 5$ h, the spectrum of filtered accelerations exhibits a deep minimum at $T \sim 10$–15 min, consistent with the structure of wind spectra (mesoscale valley) at the sea surface (e.g., [20]). There is also a slight indication of an upward trend at $T < 10$ min, corresponding to the atmospheric microscale maximum observed in the $3 < T < 0.5$ min range (e.g., [29]). The high-frequency part of the velocity spectrum is affected by the GPS noise to a much lesser extent, and exhibits a structure similar to the filtered acceleration spectrum in the high-frequency range.

To better demonstrate the filter performance, we processed the GLAD data using a much simpler technique, which removes spikes in accelerations by prescribing homogeneous motion on the respective time intervals: when $|\boldsymbol{a}_n| > a_c, \boldsymbol{r}_n$ in (11) was replaced by the value setting the numerator to zero. Compared to the proposed filter, this procedure required ten times less computer time (12 s for processing the GLAD trajectories), but provided moderate improvement of the acceleration statistics (dark gray curves in Fig. 7): the autocorrelation function is still close to the δ shape, while the spectrum appears to be homogeneously damped at high frequencies. The resulting pdf (not shown) also demonstrates an unrealistic behavior: it is abruptly cut to zero

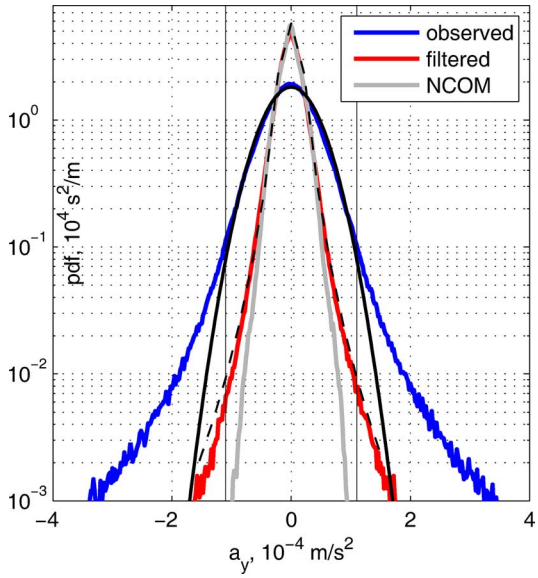

Fig. 6. Pdf of the observed GLAD drifter accelerations (blue), the Gaussian model of the accelerations induced by the GPS noise (black parabola), the pdf of the filtered accelerations (red), and the pdf of the log-normal superstatistics [2] approximating the Lagrangian accelerations observed in the laboratory experiment (the dashed line). The pdf of Lagrangian accelerations simulated by the NCOM run at 1-km resolution is given in light gray. Thin vertical lines show the value of the cutoff acceleration.

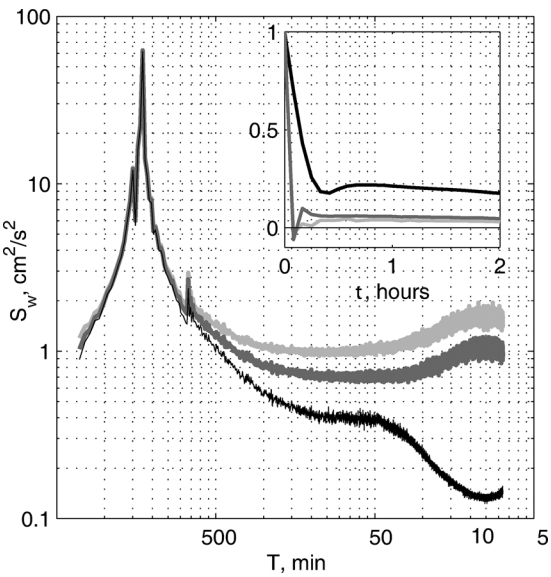

Fig. 7. Spectra of the observed (gray) and filtered (black) Lagrangian accelerations averaged over the ensemble of the GLAD trajectories. Accelerations are normalized by the local Coriolis parameter $f = 7.3 \times 10^{-5}$ s^{-1}. The structure of the corresponding autocorrelation functions near the origin is shown in the inset.

at $|a| > a_c$ and has a bulge at $a = 0$, which is the result of the accumulation of the filtered spikes. Of course, this simple algorithm can be improved (e.g., by introducing spline instead of linear interpolation), but these changes will make it noncompetitive with the proposed filter. Besides, we believe that the computational expense of the proposed filter is quite modest in a typical application involving 10^3 drifters operating during 10^2 days.

Statistical consistency with the NCOM simulations and independent experimental data indicates that the filtered trajectories are substantially more realistic in terms of the acceleration statistics. At the same time, the proposed filter has little impact on the velocity statistics because deviations of the filtered trajectories from the observed ones are relatively small and introduce only minor ($\sim$0.5–1 cm/s) corrections to the drifter velocities derived from the differences in their consecutive positions.

V. Conclusion

A method for filtering PEs from drifter trajectories is proposed. Its performance is demonstrated applying it to the GLAD data. The method is based on the assumption of the statistical independence of the PEs and Lagrangian accelerations. The PE statistics are approximated by the δ-correlated Gaussian process with time-dependent variance which prescribes higher PEs to outliers and identifies them by spikes in the acceleration time series. Statistics of drifter accelerations are specified by the stretched exponential law, whose adjustable parameter $\mu = 0.91$ is defined by optimizing *a posteriori* PE variance.

Statistics of the accelerations obtained after filtering the GLAD data are consistent with the results of high-resolution numerical simulations and is in good qualitative agreement with the typical pdf shape of the Lagrangian accelerations observed in the laboratory experiments. Quantitatively, the obtained pdf is similar to the log-normal superstatistics of Beck [2] describing the distribution of the Lagrangian accelerations observed in a developed turbulent flow [32], [33]. These results indicate potential validity of the filter when applied to other drifter data sets acquired at high temporal resolution.

It is noteworthy that a simple Gaussian assumption $\mu = 1$ on the acceleration statistics produces *a posteriori* pdf with a stronger cutoff of the tails resembling the one obtained from the NCOM model (the gray line in Fig. 6). At the same time, *a posteriori* rms deviation of the filtered trajectories from the observed ones was significantly different from the observed value $\sigma_e = 2.8$ m, because the Gaussian distribution appeared to be underdispersive. Introduction of the extra tuning parameter μ improved the situation and appears to be reasonable in the light of the cited experimental data on the Lagrangian accelerations.

The analysis also revealed that, on average, drifter positioning errors did not experience significant increase from their nominal values diagnosed ashore. This can be partly attributed to the relatively calm weather during the GLAD experiment and the sufficiently long GPS signal accumulation (5 min) between the position fixes as compared to the time scales (5–20 s) of the wave-induced disturbances.

The proposed filtering methodology can be improved in several ways. First, we did not take into account temporal correlations of the drifter accelerations along the trajectory. Second, more sophisticated distributions, such as q-exponential, or log-normal superstatistics could be used as the background pdfs for regularization of the cost function. These distributions are characterized by a sharp discontinuity at the origin ($a = 0$) and may be difficult to handle by the descent algorithms based on the assumption of differentiability of the cost function. In fact, during the search for an optimal μ, we did encounter a significant slowdown of the convergence rates at $\mu < 0.7$. Finally, the PE distribution can also be improved by updating the GPS noise model:

the PEs are likely to be correlated, at least during the sporadic events of signal loss from a significant number of satellites.

An alternative way of improving the quality of drifter data at high temporal resolution is to reduce the PEs themselves. This can be easily done in the near-coastal regions by using the existing network of the continuously operating reference stations (CORSs), which can easily deliver positions accurate to several centimeters. In the open ocean, however, this method may not work without involving a sort of bottom-referenced navigation and/or more sophisticated real-time ionosphere correction algorithms.

We consider this study to be an attempt at improving the quality of the drifter data acquired at high temporal resolution. The methodology can be extended for interpolation of the drifter positions on a regular time grid by introducing the local time-interpolation operators in the first (observational) term of the cost function. There is also plenty of room for further development of the filter along the aforementioned lines.

APPENDIX

The acceleration variance σ_a^2 is given by the integral

$$\sigma_a^2 = N \int_{-\infty}^{\infty} \int_{-\infty}^{\infty} \boldsymbol{a}^2 \exp\left[-\frac{\boldsymbol{a}^{2\mu}}{a^{2\mu}}\right] da_x da_y$$

where N is the normalization constant such that

$$N^{-1} = \int_{-\infty}^{\infty} \int_{-\infty}^{\infty} \exp\left[-\frac{\boldsymbol{a}^{2\mu}}{a^{2\mu}}\right] da_x da_y.$$

Introducing polar coordinates $a_r = |\boldsymbol{a}| = (a_x^2 + a_y^2)^{1/2}$ and $\varphi = \tan^{-1}(a_y/a_x)$ and a new variable $\eta = (a_r/a)^{2\mu}$, the normalization integral is reduced to

$$\frac{a^2}{2\mu} \int_0^{2\pi} d\varphi \int_0^{\infty} \eta^{1/\mu - 1} e^{-\eta} d\eta = \frac{\pi a^2}{\mu} \Gamma\left(\frac{1}{\mu}\right) = N^{-1} \quad \text{(A1)}$$

where the gamma function is defined by $\Gamma(s) = \int_0^{\infty} x^{s-1} e^{-x} dx$. In the similar manner, the first integral can be rewritten as

$$\sigma_a^2 = N \frac{a^4}{2\mu} \int_0^{2\pi} d\varphi \int_0^{\infty} \eta^{2/\mu - 1} e^{-\eta} d\eta = N \frac{\pi a^4}{\mu} \Gamma\left(\frac{2}{\mu}\right). \quad \text{(A2)}$$

Substitution of N from the right-hand side of (A1) into the right-hand side of (A2) yields the expression for the proportionality coefficient C in (9)

$$a^2 = \frac{\Gamma\left(\frac{1}{\mu}\right)}{\Gamma\left(\frac{2}{\mu}\right)} \sigma_a^2 \equiv C \sigma_a^2.$$

ACKNOWLEDGMENT

The authors would like to thank Dr. J. Dykes for helpful discussions.

REFERENCES

[1] C. Beck, "Dynamical foundations of nonextensive statistical mechanics," *Phys. Rev. Lett.*, vol. 87, no. 18, 2001, 180601.
[2] C. Beck, "Lagrangian acceleration statistics in turbulent flows," *Europhys. Lett.*, vol. 64, no. 2, pp. 151–157, 2003.
[3] F. J. Beron-Vera, M. J. Olascoaga, and G. J. Goni, "Oceanic mesoscale eddies as revealed by Lagrangian coherent structures," *Geophys. Res. Lett.*, vol. 35, 2008, L12603.
[4] J.-H. Bettencourt, C. Lopez, and E. Hernandez-Garcia, "Oceanic three-dimensional Lagrangian coherent structures: A study of a mesoscale eddy in the Benguela upwelling region," *Ocean Model.*, vol. 51, pp. 73–83, 2012.
[5] X. Capet, J. C. McWilliams, M. J. Molemaker, and A. F. Shchepetkin, "Mesoscale to submesoscale transition in the California Current system: Flow structure, eddy flux, and observational tests," *J. Phys. Oceanogr.*, vol. 38, pp. 29–43, 2008.
[6] X. Capet, J. C. McWilliams, M. J. Molemaker, and A. F. Shchepetkin, "Mesoscale to submesoscale transition in the California Current system: Frontal processes," *J. Phys. Oceanogr.*, vol. 38, pp. 44–64, 2008.
[7] M. E. Carr and T. Rossby, "Pathways of the North Atlantic Current from surface drifters and subsurface floats," *J. Geophys. Res.*, vol. 106, no. C3, pp. 4405–4419, 2001.
[8] R. Davis, "Drifter observations of coastal surface currents during CODE: The statistical and dynamical views," *J. Geophys. Res.*, vol. 90, no. C3, pp. 4756–4772, 1985.
[9] J. Gilbert and C. Lemarechal, "Some numerical experiments with variable-storage quasi-Newton algorithms," *Math. Programm.*, vol. 45, pp. 407–435, 1989.
[10] L. Gaultier, J. Verron, J.-M. Brankart, O. Titaud, and P. Brasseur, "On the inversion of submesoscale tracer fields to estimate the surface ocean circulation," *J. Mar. Syst.*, vol. 126, pp. 33–42, 2013.
[11] C. Harrison and G. A. Glatzmaier, "Lagrangian coherent structures in the California Current system—Sensitivities and limitations," *Geophys. Astrophys. Fluid Dyn.*, vol. 106, no. 1, pp. 22–44, 2012.
[12] B. L. Hua, J. McWilliams, and P. Klein, "Lagrangian accelerations in geostrophic turbulence," *J. Fluid. Mech.*, vol. 366, pp. 87–108, 1998.
[13] S.-Y. Kim, "Observations of submesoscale eddies using high-frequency radar-derived kinematic and dynamic quantities," *Cont. Shelf Res.*, vol. 30, pp. 1639–1655, 2010.
[14] P. M. Lee, *Bayesian Statistics: An Introduction*. New York, NY, USA: Wiley, 2012, ch. 1, ISBN: 978-1-118-33257-3.
[15] G. S. Lewis and H. L. Swinney, "Velocity structure functions, scaling, and transitions in high-Reynolds-number Couette-Taylor flow," *Phys. Rev. E*, vol. 59, no. 5, pp. 5457–5467, 1999.
[16] A. Mahadevan, A. Tandon, and R. Ferrari, "Rapid changes in mixed layer stratification driven by submesoscale instabilities and winds," *J. Geophys. Res.*, vol. 115, no. C3, 2010, DOI: 10.1029/2008JC005203.
[17] N. Mordant, E. Leveque, and J. F. Pinton, "Experimental and numerical study of the Lagrangian dynamics of high Reynolds turbulence," *New J. Phys.*, vol. 6, pp. 116–159, 2004.
[18] T. Nakamura, J. P. Matthews, T. Awaji, and H. Mitsudera, "Submesoscale eddies near the Kuril Straits: Asymmetric generation of clockwise and counterclockwise eddies by barotropic tidal flow," *J. Geophys. Res.*, vol. 117, no. C12, 2012, DOI: 10.1029/2011JC007754.
[19] T. M. Özgökmen, L. Piterbarg, A. J. Mariano, and E. H. Ryan, "Predictability of drifter trajectories in the tropical pacific ocean," *J. Phys. Oceanogr.*, vol. 31, pp. 2691–2719, 2001.
[20] W. J. Pierson, "The measurement of the synoptic scale wind over the ocean," *J. Geophys. Res.*, vol. 88, no. C3, pp. 1683–1708, 1988.
[21] A. C. Poje *et al.*, "Grand LAgrangian Deployment (GLAD): The nature of surface dispersion near the Deepwater Horizon spill," *Proc. Nat. Acad. Sci. USA*, vol. 111, no. 35, pp. 12693–12698, 2014.
[22] P.-M. Poulain, "Drifter observations of surface circulation in the Adriatic Sea between December 1994 and March 1996," *J. Mar. Syst.*, vol. 20, pp. 231–253, 1999.
[23] A. Provenzale, A. Babiano, A. Bracco, C. Pasquero, and J. B. Weiss, "Coherent vortices and tracer transport," in *Transport and Mixing in Geophysical Flows*, ser. Lecture Notes in Physics. Berlin, Germany: Springer-Verlag, 2008, vol. 744, pp. 101–118.
[24] T. Rossby, "Evolution of Lagrangian methods in oceanography," in *Lagrangian Analysis and Prediction in Coastal and Ocean Processes*. Cambridge, U.K.: Cambridge Univ. Press, 2007, pp. 1–38.
[25] B. G. Sanderson and D. A. Booth, "The fractal dimension of drifter trajectories and estimates of horizontal eddy-diffusivity," *Tellus*, vol. 43A, pp. 334–349, 1991.

[26] R. B. Scott *et al.*, "Estimates of surface drifter trajectories in the equatorial Atlantic: A multi-model ensemble approach," *Ocean Dyn.*, vol. 62, pp. 1091–1109, 2012.
[27] E. van Sebille, P. J. van Leeuwen, A. Biastoch, C. N. Barron, and W. P. M. de Ruijter, "Lagrangian validation of numerical drifter trajectories using drifting buoys: Application to the Agulhas system," *Ocean Model.*, vol. 29, pp. 269–276, 2009.
[28] L. N. Thomas, A. Tandon, and A. Mahadevan, "Submesoscale processes and dynamics," in *Ocean Modeling in an Eddying Regime*, ser. Geophysical Monograph. New York, NY, USA: Wiley, 2008, vol. 177, pp. 17–38.
[29] N. K. Vinnichenko, "The kinetic energy spectrum in free atmosphere—1 second to 5 years," *Tellus*, vol. 12, no. 2, pp. 158–166, 1970.
[30] R. Volk *et al.*, "Acceleration of heavy and light particles in turbulence: Comparison between experiments and direct numerical simulations," *Physica D*, vol. 237, no. 14–17, pp. 2084–2089, 2008.
[31] A. G. Zatsepin *et al.*, "Submesoscale eddies at the Black Sea shelf and the mechanisms of their generation," *Oceanology*, vol. 51, no. 4, pp. 554–567, 2011.
[32] A. La Porta, G. A. Voth, A. M. Crawford, J. Alexander, and E. Bodenschatz, "Fluid particle accelerations in fully developed turbulence," *Nature*, vol. 409, pp. 1017–1019, 2001.
[33] G. A. Voth, A. La Porta, A. M. Crawford, J. Alexander, and E. Bodenschatz, "Measurement of particle accelerations in fully developed turbulence," *J. Fluid. Mech.*, vol. 469, pp. 121–160, 2002.

Max Yaremchuk received the Ph.D. degree in aerodynamics and thermodynamics from the Moscow Institute of Physics and Technology, Moscow, Russia, in 1984.

His research is focused on the development of inverse methods of data processing using variational and ensemble technics.

Emanuel F. Coelho received the Ph.D. degree in physical oceanography from the Naval Postgraduate School, Monterey, CA, USA, in 1994.

His present research interests include environmental stochastic modeling, nonlinear filtering theory and control theory applied to environmental adaptive decision, risk management, and data assimilation.